Nonlinear control-based robust voltage regulation of a magnetically coupled multiport dc-dc power converter for automotive applications

David Aquilué Llorens and David París Escarcelle
Enginyeria Física
Universitat Politècnica de Catalunya
(Dated: June 19, 2020)

This paper presents two different control strategies to regulate the output voltage of a magnetically coupled multiport dc-dc converter aimed at automotive applications. The two models, a feedback linearizing and an adaptive control-based, guarantee asymptotic stability in the face of resistive load and constant power load variations and their performances are verified through numerical simulations. The two controllers are compared, and an integral action is added to the adaptive scheme and tested.

I. INTRODUCTION

Over the past few years, electrified systems have increasingly been applied in the automotive sector since they provide an improved driving experience. This electrification does not only apply to electric power trains but also to transmission and chassis electronics, driver assistance, passive safety or comfort and entertainment systems. As a consequence, implementation of on-board dc micro-grids is a matter of high interest, more precisely the solution of issues regarding stability when facing CPL's efficiency and robustness.In this work the control design of a dc multi-bus with three of the most used voltages in automotive applications has been studied.

II. MATHEMATICAL MODEL

The three dc buses provide 400V for the power train and 48V and 12V for other auxiliary uses. These voltages are delivered to the different devices by a magnetically coupled multiport dc-dc converter which consists of a high frequency transformer with three ports connected to a full-bridge converter in parallel with a capacitor in the dc side each.

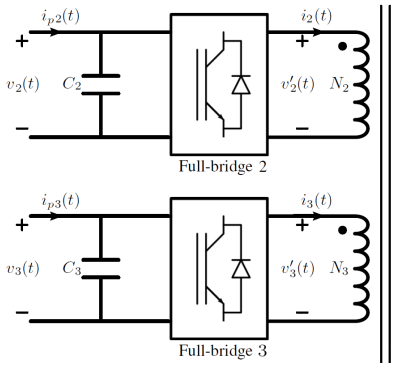

FIG. 1. Multiport dc-dc converter scheme, from [1]

The following equations describe the voltage dynamics of the three ports:

$$C_k\dot{v_k} = i_{pk} - \frac{1}{w_1}\sum_{l=1,l\neq k}^{3}\frac{v_l}{\alpha_{kl}L'_{kl}}\delta_{kl}\left(1-\frac{|\delta_{kl}|}{\pi})\right), \quad (1)$$

where for $k = 1, 2, 3$, v_k, are the dc voltages, i_{pk} the dc currents, C_k are the capacitors, $w_1 = \frac{2\pi}{T}$ is the fundamental frequency of the periodic voltages and currents in the transformer, α_{kl} is the transformer turn ratio of the k-th port with respect to the l-th port, L'_{kl} is the meshed-transformed linking inductance between port k and any l-th port, and $\delta_{kl} = \theta_l - \theta_k$ where the θ_i are the phase shifts of the modulated voltages. Even though the system consists of three different dc buses, the voltage at the 400V bus is assumed to be constant(because of the high capacity battery in this bus) while the two others have several loads connected to them. Setting $\theta_1 = 0$ the system dynamics (see Fig. 1) are described by:

$$\begin{aligned} C_2\dot{v_2} = &-\frac{v_2}{R_2} - \frac{P_2}{v_2} + \frac{E_1}{w_1\alpha_{12}L'_{12}}\theta_2\left(1-\frac{|\theta_2|}{\pi}\right) + \\ &-v_3\frac{1}{w_1\alpha_{23}L'_{23}}(\theta_3-\theta_2)\left(1-\frac{|\theta_3-\theta_2|}{\pi}\right) \end{aligned} \quad (2a)$$

$$\begin{aligned} C_3\dot{v_3} = &-\frac{v_3}{R_3} - \frac{P_3}{v_3} + \frac{E_1}{w_1\alpha_{13}L'_{13}}\theta_3\left(1-\frac{|\theta_3|}{\pi}\right) + \\ &+v_2\frac{1}{w_1\alpha_{32}L'_{32}}(\theta_3-\theta_2)\left(1-\frac{|\theta_3-\theta_2|}{\pi}\right). \end{aligned} \quad (2b)$$

where v_2 is the voltage of the 48 V bus, v_3 is the voltage of the 12 V bus, and the phase shifts in ports 2 and 3, θ_2 θ_3, respectively, are going to be used as control variables. The control objective is to bring the v_2 and v_3 voltages to their value of reference, $v_2^* = 48V$ and $v_3^* = 12V$.

III. FEEDBACK LINEARIZING CONTROL

In this section an adequate change of variables will be used to linearize and decouple the system with the objective of designing a stable PI controller.

A. Control Algorithm

Some of the next algebraic manipulations will be skipped for brevity. Let $f_2(\theta_2)$, $f_3(\theta_3)$, λ_2, λ_3 and

$g(\theta_2, \theta_3)$ be defined [1] such that (2) can be written as:

$$C_2\dot{v_2} = -\frac{v_2}{R_2} - \frac{P_2}{v_2} + f_2(\theta_2) - \lambda_2 v_3 g(\theta_2, \theta_3) \tag{3a}$$

$$C_3\dot{v_3} = -\frac{v_3}{R_3} - \frac{P_3}{v_3} + f_3(\theta_3) - \lambda_3 v_2 g(\theta_2, \theta_3). \tag{3b}$$

Then, the following change of state and control variables is proposed:

$$\xi_2 = v_2^2, \quad \xi_3 = v_3^2 \tag{4a}$$

$$u_2 = f_2(\theta_2) - \lambda_2 v_2 v_3 g(\theta_2, \theta_3) \tag{4b}$$

$$u_3 = f_3(\theta_3) + \lambda_3 v_2 v_3 g(\theta_2, \theta_3). \tag{4c}$$

The system dynamics results in a linear, decoupled system with state variables ξ_2, ξ_3.

$$\dot{\xi_i} = -\frac{2}{R_i C_i}\xi_i - \frac{2P_i}{C_i} + \frac{2}{Ci}u_i. \quad i = 2, 3. \tag{5}$$

Considering the PI controller:

$$u_i = -k_{pi}\xi_i + k_{zi} z_i \tag{6a}$$

$$\dot{z_i} = \xi_i^* - \xi_i, \tag{6b}$$

with $\xi_2^* = 48^2$ and $\xi_3^* = 12^2$ the closed loop system is given by:

$$\dot{\xi_i} = -\frac{2}{C_i}\left(\frac{1}{R_i} + k_{pi}\right)\xi_i - \frac{2P_i}{C_i} + \frac{2k_{zi}}{Ci} z_i. \tag{7}$$

The equilibrium point, $(xi_2^*, z_2^*, xi_3^*, z_3^*)$, and characteristic polynomial can be straightforwardly calculated from the error dynamics, and global asymptotic stability is guaranteed for:

$$\frac{1}{R_i} + k_{pi} > 0, \quad k_{zi} > 0, \quad i = 2, 3, \tag{8}$$

proving the system to be robust for uncertainties in the values of R_i and P_i.
The main problem with this control law is the inversion of the change of variables, which is analyzed in Section IV of [1].

B. Simulation Results

For the simulations the Matlab function *ode45* with a tolerance of 10^{-4} has been used to solve the differential equation. The following profiles have been defined, respectively, for R_i and P_i:

$$R_2 = \begin{cases} 5\Omega & t \in [0, 0.03) \cup [0.05, 0.1)s \\ 3\Omega & t \in [0.03, 0.05)s \end{cases} \tag{9}$$

$$R_3 = \begin{cases} 10\Omega & t \in [0, 0.04) \cup [0.06, 0.1)s \\ 3\Omega & t \in [0.04, 0.06)s, \end{cases} \tag{10}$$

$$P_2 = \begin{cases} 0 & t \in [0, 0.065)s \\ 2kW & t \in [0.065, 0.1)s \end{cases} \tag{11}$$

$$P_3 = \begin{cases} 0 & t \in [0, 0.075)s \\ 100W & t \in [0.075, 0.1)s. \end{cases} \tag{12}$$

The controller gains k_{p2}, k_{z2}, k_{p3} and k_{z3} have been iteratively adjusted seeking for a trade off between relative error and computational time. Figures 1 and 2 depict the voltages tracking their respective references for three sets of control gains. In Figure 2 the voltage of the 12V bus for the two sets of gains has been omitted since the tracking was almost perfect, with only a barely noticeable ripple.
It has been observed that the larger the controller gains, the larger the computational time but also the smaller the error. However, one has to take into account that such gains are limited by the characteristics of the controller when it is applied to a real-life scenario.

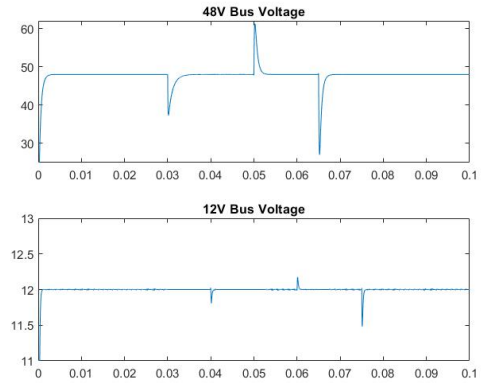

FIG. 2. Voltages of the 48V and 12V buses for $k_{p2} = 0.8$, $k_{z2} = 1640$, $k_{p3} = 6$ and $k_{z3} = 3033$.

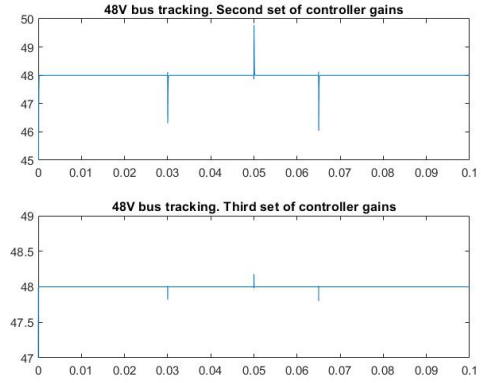

FIG. 3. Top: 48V bus for $k_{p2} = 8$, $k_{z2} = 164e3$, $k_{p3} = 60$ and $k_{z3} = 303300$. Bottom: 48V bus for $k_{p2} = 80$, $k_{z2} = 164e5$, $k_{p3} = 60$ and $k_{z3} = 3033e4$.

IV. ADAPTIVE CONTROL

In this section, the strategy presented to regulate the micro-grid output voltage is an observer-based adaptive control law. For this purpose, we will use the same coupled equations (3) as in the feedback linearizing. The following change of control variables is proposed:

$$u_2 = v_2 f_2(\theta_2) - \lambda_2 v_3^* g(\theta_2, \theta_3) \tag{13a}$$
$$u_3 = v_3 f_3(\theta_3) + \lambda_3 v_2^* g(\theta_2, \theta_3). \tag{13b}$$

Then, observers regarding conductances and CPLs are included to obtain asymptotic voltage regulation and robustness to the resistive load changes. Finally, stability is proved using LaSalle's invariance principle [2] and numerical simulations are presented to validate the method.

A. Control Algorithm

As before, the control goal is to regulate the dc voltages to the reference values, $v_2^* = 48V$, $v_3^* = 12V$, considering variations in the conductance and CPL in the buses: G_k and P_k. Let $\hat{G}_k$ and $\hat{P}_k$ denote their estimation values and $e_k = v_k - v_k^*$ denote the error variables. The adaptive control law is defined as:

$$u_k = \hat{G}_k(e_k + v_k^*) + \frac{\hat{P}_k}{e_k + v_k^*} - \gamma_k e_k, \tag{14a}$$
$$\dot{\hat{G}}_k = -\frac{\mu_k}{\lambda_k} e_k (e_k + v_k^*), \tag{14b}$$
$$\dot{\hat{P}}_k = -\frac{\nu_k e_k}{\lambda_k (e_k + v_k^*)}, \tag{14c}$$

and the set of equations (3) boil down to:

$$C_2 \dot{e_2} = -\Delta G_2 (e_2 + v_2^*) - \frac{\Delta P_2}{e_2 + v_2^*} - \lambda_2 e_3 H(u) - \gamma_2 e_2, \tag{15a}$$
$$C_3 \dot{e_3} = -\Delta G_3 (e_3 + v_3^*) - \frac{\Delta P_3}{e_3 + v_3^*} + \lambda_3 e_2 H(u) - \gamma_3 e_3, \tag{15b}$$
$$\dot{\Delta G}_k = \frac{\mu_k}{\lambda_k} e_k (e_k + v_k^*), \tag{15c}$$
$$\dot{\Delta P}_k = \frac{\nu_k e_k}{\lambda_k (e_k + v_k^*)}. \tag{15d}$$

with $\Delta G_k = G_k - \hat{G}_k$, $\Delta P_k = P_k - \hat{P}_k$ and γ_k, μ_k, ν_k, $\in \mathbb{R}^+$, $k = 2, 3$, makes the closed-loop system locally stable and $e_k \to 0$, when $t \to +\infty$. The inversion of the control law is performed from its linear approximation [2].

B. Simulation results

The previous equations and parameters have been modeled using Matlab and the equations have been solved with *ode45*, with a tolerance of 10^{-5}. The system has been put under the same resistance and constant power load changes as the feedback linearizing. Resistance load changes are seen in the following graphics as the two first spikes in each voltage. Furthermore, CPL changes are observed as the third spike in both voltage graphics. The spikes represent the external variations of the system, and it is seen that the response of the system is the desired. Graphics representing the evolution of the conductance and CPL observers and the control actions are available in Figures 4, 5, 6.

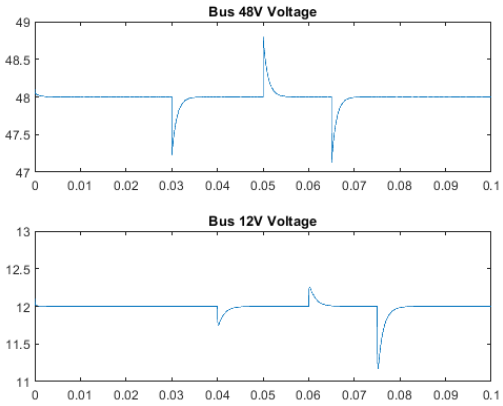

FIG. 4. Voltages of the 48V and 12V buses.

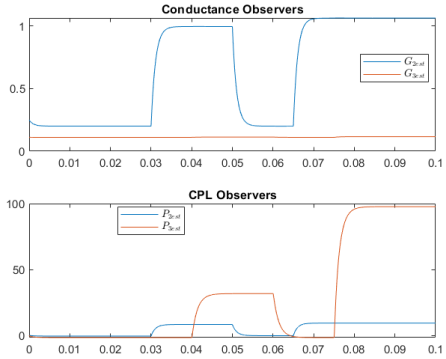

FIG. 5. Conductance and CPL observers.

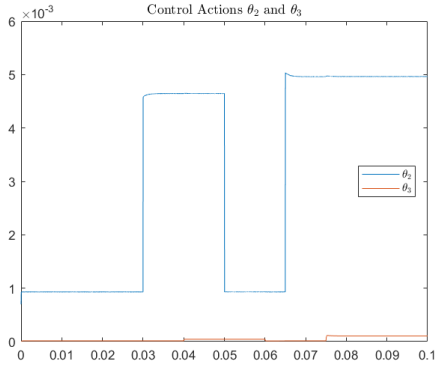

FIG. 6. Control actions θ_1 and θ_2.

V. ADAPTIVE CONTROL WITH INTEGRAL ACTION

Finally, the objective is to improve the adaptive controller described in the last section by including and integral action $\rho_k z_k$ in the control law. All the nomenclature related to this case is exactly the same as in the simple adaptive. The control law is described as:

$$u_k = \hat{G}_k(e_k + v_k^*) + \frac{\hat{P}_k}{e_k + v_k^*} - \gamma_k e_k - \rho_k z_k, \tag{16a}$$

$$\dot{\hat{G}}_k = -\frac{\mu_k}{\lambda_k} e_k(e_k + v_k^*), \tag{16b}$$

$$\dot{\hat{P}}_k = -\frac{\nu_k e_k}{\lambda_k(e_k + v_k^*)}, \tag{16c}$$

$$\dot{z}_k = e_k, \tag{16d}$$

and the set of equations in (3) now yields:

$$C_2\dot{e_2} = -\Delta G_2(e_2 + v_2^*) - \frac{\Delta P_2}{e_2 + v_2^*} - \lambda_2 e_3 H(u) + \\ -\gamma_2 e_2 - k_2 z_2 \tag{17a}$$

$$C_3\dot{e_3} = -\Delta G_3(e_3 + v_3^*) - \frac{\Delta P_3}{e_3 + v_3^*} + \lambda_3 e_2 H(u) + \\ -\gamma_3 e_3 - k_3 z_3, \tag{17b}$$

$$\dot{\Delta G}_k = \frac{\mu_k}{\lambda_k} e_k(e_k + v_k^*), \tag{17c}$$

$$\dot{\Delta P}_k = \frac{\nu_k e_k}{\lambda_k(e_k + v_k^*)}. \tag{17d}$$

with $\Delta G_k = G_k - \hat{G}_k$, $\Delta P_k = P_k - \hat{P}_k$ and γ_k, μ_k, ν_k, $\in \mathbb{R}^+$, $k = 2, 3$, makes the closed-loop system locally stable and $e_k \to 0$, when $t \to +\infty$. To prove the stability of this controller, we introduce the auxiliary function V:

$$V = \frac{1}{2}\sum_{k=2}^{3}\left(\frac{C_k}{\lambda_k}e_k^2 + \frac{1}{\mu_k}\Delta G_k^2 + \frac{1}{\nu_k}\Delta P_k^2 + \frac{\rho_k}{\lambda_k}z_k^2\right), \tag{18}$$

which, with $\frac{\rho_k}{\lambda_k} > 0$ is positive definite. Its derivative:

$$\dot{V} = \sum_{k=2}^{3}\left(\frac{C_k}{\lambda_k}e_k\dot{e}_k + \frac{1}{\mu_k}\Delta G_k\dot{\Delta G}_k + \frac{1}{\nu_k}\Delta P_k\dot{\Delta P}_k \right. \\ \left. + \frac{\rho_k}{\lambda_k}z_k\dot{z}_k\right) = \sum_{k=2}^{3} -\frac{\gamma_k}{\lambda_k}e_k^2, \tag{19}$$

is ≤ 0. Moreover, the subset of $\mathbb{R}^8$ where $\dot{V}$=0 is

$$\Omega_R = \{(0, 0, \Delta G_2, \Delta G_3, \Delta P_2, \Delta P_3, z_2, z_3)\}$$

while the largest invariant set within Ω_R is

$$\Omega_R = \{(0, 0, \Delta G_2^*, \Delta G_3^*, \Delta P_2^*, \Delta P_3^*, z_2^*, z_3^*), \\ \Delta P_k^* = -\Delta G_k^* v_k^{*2} - k_k z_k^* v_k^*\}$$

Then, La Salle's invariance principle ensures that, locally, the trajectories of (17) tend to Ω when $t \to +\infty$.

A. Simulation results

As in the other controllers, simulations using Matlab and *ode45* with a tolerance of 10^{-5} have been performed. The system has been put under the same resistance and constant power load changes as the other two. For values of $k_2 = [50,100]$ and $k_3 = [0.5,2]$, the results were the same as for the simple adaptive.
The system analyzed until now is a simplification of a real system. This way, the effects that appear in a real-life scenario which would alter the steady state are not present so the integrator has no effect.
A more realistic model of the system has been analyzed with SimuLink which includes non-ideal effects such as losses in the power switches or reactive components.

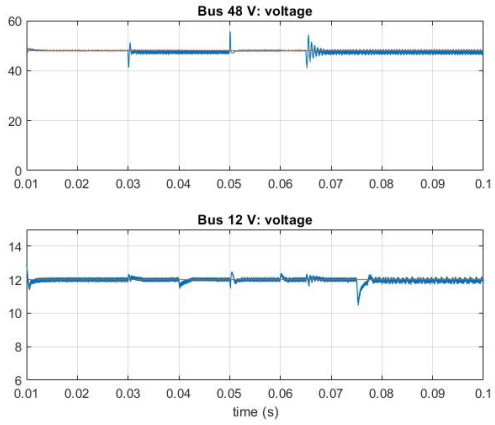

FIG. 7. Bus voltages (blue) and voltage references (red) for 48V and 12V buses.

However, once again, no significant improvement has been observed when using the integral action with respect to the basic adaptive control (refer to the plots in Section IV of [2]).
From the set of equations 16, the adaptive control variable u_k with integral action can be written as:

$$u_k = -\gamma_k e_k - \frac{\mu_k}{\lambda_k}(e_k + v_k^*)\int_0^t e_k(e_k + v_k^*) + \\ -\frac{v_k}{\lambda_k(e_k + v_k^*)}\int_0^t \frac{e_k}{(e_k + v_k^*)} - \rho_k\int_0^t e_k. \tag{21}$$

One can see that even without the effect of the integral action ($\rho_k = 0$), the adaptive control law behaves similarly to what could be described as a non-linear PI controller, it already takes into account the amount of error accumulated over time, which would make sure that e_k approaches zero when time increases. For this reason, the effect of the integral action does not improve significantly the already small steady state error.

Citations and References

[1] Josep M. Olm, Enric Fossas, Victor Repecho, Arnau Doria-Cerezo and Robert Griñó, "Feedback linearizing

control of a magnetically coupled multiport dc-dc converter for automotive applications", Proc. of the 45th Annual Conference of the IEEE Industrial Electronics Society (IECON), pp. 2688-2693, 2019.

[2] Josep M. Olm, Enric Fossas, Victor Repecho, Arnau Doria-Cerezo and Robert Griñó, "Adaptive control-based voltage regulation of a magnetically coupled multiport dc-dc converter for electrified vehicles", IEEE International Symposium on Circuits and Systems (ISCAS), 2020.